Peer-reviewed version available at Construction and Building Materials 2019, 209, 541-547; doi:10.1016/j.conbuildmat.2019.03.068

Correlations between air permeability coefficients and pore structure indicators of cementitious materials

Yuya Sakai[1]*
Institute of Industrial Science, The University of Tokyo
ysakai@iis.u-tokyo.ac.jp

Abstract
Correlations between the air permeability coefficient and various pore structure indicators in cementitious materials were examined to determine the pore structure indicator that best evaluated air permeability using data from previous studies of air permeabilities and pore structures. The determination coefficients of air permeability with total pore volume, critical pore diameter, and ordinary threshold pore diameter were low, although these have often been used as indicators. The median and threshold pore diameters obtained by percolation theory showed high determination coefficients. The equation using the threshold pore diameter better estimated the air permeability coefficient than the Katz–Thompson equation.

Keywords: air permeability, total pore volume, critical pore diameter, threshold pore diameter, median pore diameter, Katz–Thompson equation

Highlights

- Air permeability and pore structure of cementitious materials are closely related
- Data from reports on air permeability and porosity in cements were analysed
- Percolation theory-derived threshold pore diameter gives the best estimates
- Proposed equation yields better results than Katz–Thompson relationship

1. Introduction

The air permeability coefficient of concrete is important in evaluating the durability of concrete structures because the permeation of carbon dioxide and oxygen into concrete causes deterioration by carbonation and corrosion of reinforcement bars. Researchers have studied the relationship between the air permeability coefficient and the pore structures of concrete to understand the transportation mechanism of air and establish models that predict the air permeability of concrete; various characteristic indicators of the pore structure have been proposed. Among indicators characterising pore structure, the relationship between the total pore volume and air permeability has been reported the most extensively. The total pore volume is generally measured in one of three ways: calculation using the difference between the water-saturated and oven-dried weights [1–3], the maximum volume of cumulative intruded mercury in mercury intrusion porosimetry (MIP) [4–6], and image analysis of the area fraction of pores [7,8]. Some researchers set maximum and minimum pore sizes in calculating the total pore volume [9,10] without clear theoretical reason. However, as Diamond [11] noted, the pore size distribution obtained by MIP is not a true pore size distribution because of ink-bottle effects; the validity of using a total porosity with certain maximum and minimum pore sizes is unclear.

Hamami et al. [12] used the main pore diameter D_c, defined as the mean value of the normal distribution fitted on the main peak of a pore size distribution, as an indicator of the pore structure and reported that the square of D_c multiplied by the total pore volume fraction φ showed good correlation with the air permeability coefficient. This method can be difficult to apply because the pore size distribution of concrete can be far from a normal distribution, as shown in Fig. 1. Zhang et al. [13] studied the relationships between the air permeability coefficient and various pore structure indicators, including the median pore diameter. The median pore diameter is defined as the corresponding pore diameter when the volume of press-in mercury is 50% of the maximum volume of the cumulative intruded mercury. Tsivilis et al. [14] reported that the mean pore diameter correlated well with the air permeability. The equation for calculating the mean pore diameter can be found in Ref. [13]. Mizuno et al. [15] performed MIP on hardened cement pastes twice to obtain a continuous pore size distributions. They reported a better correlation of the total pore volume and mean pore diameter of

the continuous pores with the air permeability coefficient. Although good correlations with air permeability were reported in each of the above papers, the mentioned indicators of pore structure are not often used.

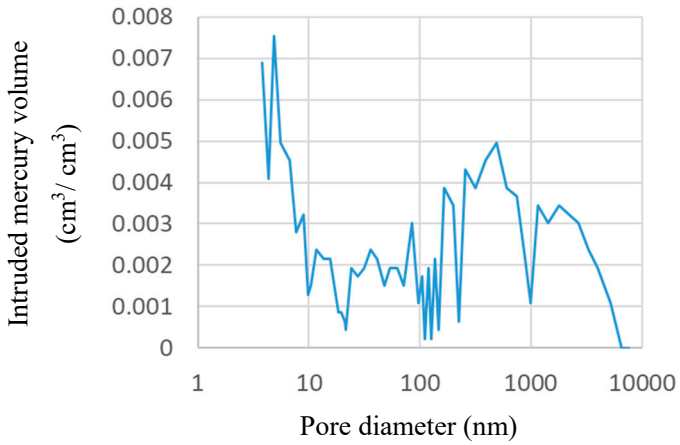

Fig. 1. Pore size distribution of concrete far from a normal size distribution (data of cored concrete from existing structure in Sakai and Kishi [16])

The critical pore diameter and threshold pore diameter are the most frequently used characteristic indicators of pore structures. The critical pore diameter is defined as the pore diameter above which a connected path is formed from one side of the sample to the other [17]. Mathematically, the critical pore diameter corresponds to the maximum of the derivative of the pore size distribution curve [18], or to the inflection point of a cumulative pore distribution curve [19]. For hardened cement paste, the maximum of the pore distribution curve and the inflection point of the cumulative pore distribution curve are clear; however, for concrete, multiple peaks often exist, impeding the determination of the critical pore diameter (Figs. 1 and 2). Roy [20] reported that the critical pore diameter and median pore diameter had similar values. The threshold pore diameter is another frequently used indicator defined similarly; however, researchers have not yet agreed on a method to determine it [21]. Various mathematical definitions of the threshold pore diameter have been proposed, including the intersection point between the tangent line of the mutational point of the slope of the curve and the pore-diameter abscissa [18], the largest pore diameter at which a significant intruded pore volume is detected, the pore diameter at which the slope of the cumulative curve increases abruptly [21,22], or the intersection point of the two straight fitting lines obviously below and above the threshold pore diameter [21]. However, determining the threshold pore diameter of concrete is difficult because the abrupt intrusion and inflection point are often unclear (Fig. 3).

Preprints (www.preprints.org) | NOT PEER-REVIEWED | Posted: 6 December 2018 doi:10.20944/preprints201812.0078.v1

Peer-reviewed version available at Construction and Building Materials 2019, 209, 541-547; doi:10.1016/j.conbuildmat.2019.03.068

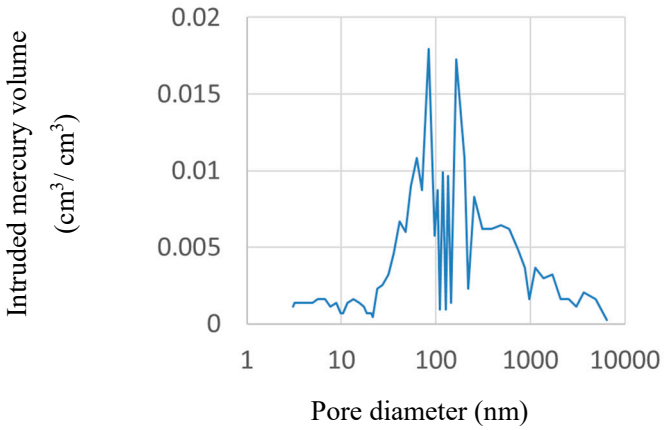

Fig. 2. Multiple peaks in pore size distribution of concrete (data of concrete sample N70-1 in Sakai et al. [23])

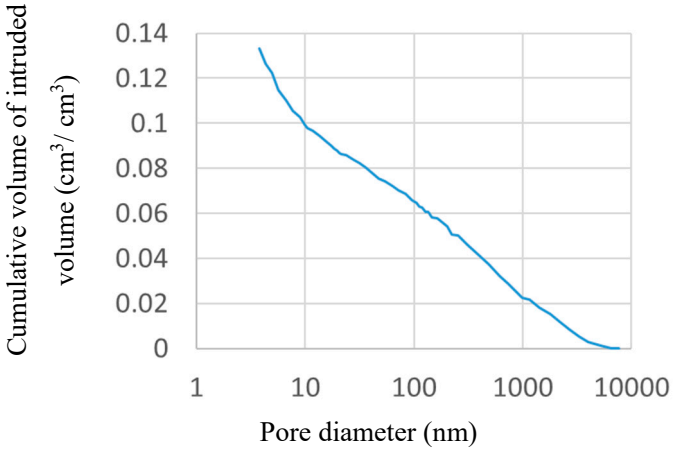

Fig. 3. Unclear abrupt intrusion and inflection point for concrete pore distribution (data of cored concrete from existing structure in Sakai and Kishi [16])

As seen, although the critical pore diameter and threshold pore diameter are widely used as indicators of the pore structure, they are difficult to determine for concrete specimens. Sakai et al. [23] proposed a method to determine the threshold pore diameter based on percolation theory, assuming that a connected path was formed when the volume of the intruded mercury reached 16% of the cement paste volume [24,25], wherein the corresponding pore size was the threshold pore diameter. They showed that their method was applicable to concrete.

In addition to the correlations between air permeability and pore structure indicators introduced above, models to calculate the air permeability coefficient based on theory have been proposed. Carman proposed the following equation [19,26]:

$$k = \frac{\varphi^2}{b \cdot S^2} \quad (1)$$

where k is the air permeability coefficient, φ is the total pore volume fraction, S is the specific surface area, and b is a sample-dependent coefficient. Kohno and Ujike [27] proposed a model to calculate the air permeability coefficient of an unsaturated sample using the saturation degree and tortuosity. Their model requires the measured air permeability coefficient and the total pore volume of the dry sample. One disadvantage of the above models is that a preliminary air permeability test is required to calculate the air permeability coefficient.

Katz and Thompson [28,29] and Thompson et al. [30] proposed the following equations to calculate the air permeability coefficient of a porous rock sample using the critical pore diameter, based on percolation theory:

$$k = \frac{1}{226} \cdot \frac{\sigma}{\sigma_0} \cdot d_c^2 \quad (2)$$

$$\frac{\sigma}{\sigma_0} = \frac{d_{max}^e}{d_c} \cdot \varphi \cdot S(d_{max}^e) \quad (3)$$

where σ is the conductivity of the rock saturated with a brine solution having the conductivity σ_0, d_c is the critical pore diameter, d_{max}^e is the electrical conductivity characteristic dimension that produces the maximum conductance ($d_{max}^e = 0.34 \times d_c$ for a very broad pore size distribution), and $S(d_{max}^e)$ is the fractional volume of the connected pore space involving pores of $>d_{max}^e$. This equation is advantageous because none of the parameters require preliminary air permeability testing. Researchers have applied this equation to cementitious materials; some have concluded that they are suitable for cementitious materials [18,19,31], but others have reported otherwise [17]. Ma [21] proposed the use of the characteristic pore diameter, which is 3–5 nm, instead of the critical pore diameter for specimens in which φ is below a certain value.

As seen above, various pore structure indicators and equations have been proposed and their correlations with the air permeability coefficient have been studied. However, in verifying the indicators or the equations, all researchers have used only their own data or limited data from other reports. When poor correlations were found, some adjustments have been proposed with probable explanations. Thus, the pore structure indicator and equation that are the best for correlating or estimating air permeability remain unknown. This must be rectified to understand the mechanism of air transport in concrete and to estimate the durability of concrete with accuracy. This study sourced data from previous reports that measured both the air permeabilities and pore structures of cementitious materials and analysed them to determine the indicator of pore structure characteristics and equation that yields the best approximation of air permeability. This report does not discuss the mechanism of air transport based on the results, because the papers that proposed each indicator have already done so.

2. Methods

In this investigation, literature that measured the air permeability coefficient and pore size distribution or pore structure indicators such as the median, critical, and threshold pore diameters was analysed. For a differential or cumulative pore size distribution from such literature, the pore structure indicators obtainable from this distribution were read using GSYS software (Japan Charged-Particle Nuclear Reaction Data Group, Japan). When intrusion steps appeared clearly in these distributions, the graphs were read using the software and differential and cumulative pore size distributions were each converted into the other. The threshold pore diameter was determined as the intersection point of the two straight fitting lines for the diameters obviously below and above the threshold pore diameter [21] and as the corresponding pore diameter when the volume of the intruded mercury corresponded to 16% of the cement paste volume [23].

The collected literature data are shown in Table 1. In the table, the information given by each study is shown as A, B, or C, indicating that the values are either reported in figures, obtainable from figures, or unpublished, respectively. The pore volume per unit mass (e.g.: mL/g) was converted to the pore volume per unit volume (φ) using the bulk density, calculated by the following equations:

$$\varphi = \varphi_m \cdot \rho_a \quad (4)$$

$$\rho_a = \frac{1}{\frac{1}{\rho_t} + \varphi_m} \quad (5)$$

where ρ_a is the bulk density, ρ_t the true density, and φ_m the total pore volume per unit mass. ρ_t was assumed as 2.7 g/cm^3 and 2.3 g/cm^3 for cement paste and mortar, respectively. When the units of air permeability coefficient are length over time (e.g. cm/s), they are converted to square meters (m^2) by multiplying by the air viscosity (0.0000183 Pa·s) and dividing by the air weight per unit volume (12.6714 N/m^3). The Katz–Thompson equation [28–30] was applied to calculate the air permeability coefficient when both the total pore volume and critical pore diameter were available.

153 Table 1 List of testing conditions in the literatures used for analysis.

Ref.	MIP						Specimen	Air permeability test		
	C. dist.	D. dist.	Cr	T1	T2	M		Unit	Pressure (kPa)	Drying procedure
10		A	B	B	B	B	Concrete	cm/s	160	20 °C and 60% RH until constant mass
12		A	B	B	B	B	Paste mortar	m^2	150–250	45 °C for 19 weeks and 80 °C
13			A	A		A	Concrete	m^2	150–350	Following RILEM TC 116-PCD
15	A		B	B	B	B	Paste	m^2	300–500	Vacuum for 2 months
16			C	C	A	C	Concrete	m^2	−98	Outside under roof
23			C	C	A	C	Concrete	m^2	−98	20 °C for 3 years
27				A			Concrete	$cm^4/N{\cdot}s$	200	50 °C until constant mass
32	A		B	B	B	B	Concrete	m^2	500	40 °C for >3 weeks
33	B	A	B	B	B	B	Concrete	m^2	150–600	105 °C for 2 days
34		A	B	B	B	B	Concrete	cm/s	200	20 °C for 12 months
35	A	B	B	B	B	B	Concrete	m^2	−98	Outside under roof

154 C. dist.: Cumulative pore size distribution, D. dist.: differential pore size distribution
155 Cr, T1, T2, and M: critical pore diameter, ordinary threshold, proposed threshold, and median pore diameter
156 A: reported in the literature, B: read from the literature, C: unpublished data, Empty: N/A

157

158 To study the relationship between air permeability and pore structure, the saturation degrees of the
159 specimens should be similar because insufficient drying reduces the air permeability with the retention
160 of moisture. Therefore, in this paper, only data from studies that conducted air permeability testing
161 with sufficiently dried specimens are used; others are omitted. For example, the studies using
162 specimens dried at 20 °C for 28 days [36,37] are not included. Some studies show the pore size
163 distribution as histograms [34] or cumulative bar charts [9]. The data range of the cumulative bar chart
164 reported by Azuma et al. [9] is wide, from which it is difficult to obtain accurate pore structure
165 indicators; therefore, this study is excluded from the table. Many papers reported the air permeability
166 coefficient using only the total pore volume as an indicator of pore structure [1–6,8,38]; these are
167 excluded from the list, because otherwise the number of plots of total pore volume versus air
168 permeability coefficient would be considerably larger than those of other pore structure indicators,
169 impeding a fair comparison. For the pore size distributions reported by Mizuno et al. [15], two
170 distributions (from samples 60B30 and 60B60) agree completely despite their different mix
171 proportions. Because the total pore volume of sample 60B60 from their figure differs from that
172 reported in a table in their paper, the data for 60B60 was likely a mistake and therefore removed.
173 In Table 1, the drying conditions before air permeability testing, applied pressures for air permeability
174 testing, and units of the reported air permeability coefficients are also shown. In the collected studies,
175 some tests were conducted with pressurised air, while others were conducted in a vacuum. Because
176 the mechanism of air transport and the air permeability coefficient are changed depending on the test
177 pressure, removing the effect of pressure is preferred before examining the correlation between the air
178 permeability and pore structure. Hamami et al. [12] plotted the relationship of air permeability
179 coefficients with the inverses of the testing pressures and reported the intersection of the regression
180 line of the data with the longitudinal axis as the intrinsic air permeability coefficient. This air
181 permeability corresponds to the data measured at an infinitely high pressure. To remove the effect of
182 pressure, air permeability testing must be performed at multiple pressures; however, in most of the
183 analysed studies, the pressure dependence of the air permeability was not investigated. Therefore, the
184 data in these other works cannot be adjusted, and although the air permeability tests in the works

summarised in Table 1 were performed at different pressures, the effect of pressure was not removed. According to a figure (Fig. 6) in Hamami et al. [12], the measured air permeability coefficient they reported might be a few times larger than the reported intrinsic air permeability coefficient. The pressure range of the air permeability tests summarised in Table 1 is −98 to 500 kPa. The air permeability measured at high pressure becomes larger for samples tested at atmospheric pressure; that tested at low pressure (i.e. vacuum) becomes smaller at atmospheric pressure [39]. The pressure dependence of the air permeability coefficient increases as the pore diameter decreases; at the pore diameter of 10 nm, the air permeability coefficients at −98 kPa and 300 kPa can vary by a factor of three [39]. These pressure dependences should be considered in discussing the correlations between air permeability and characteristic pore structure collected from various studies. However, the results shown in Section 3 are presented in the logarithmic scale, and differences of factors of <3 do not introduce problems in studying the correlations.

3. Results and discussion

The reported and calculated air permeability coefficients; total pore volumes; and median, critical, and threshold pore diameters are shown in Figs. 4–8 with approximation curves. The approximation curves in the figures are drawn assuming exponential approximations unless otherwise noted. Fig. 4 shows the relationship between the air permeability coefficient and total pore volume; the approximation curve is drawn assuming a logarithmic approximation. In most studies, mercury is intruded to the pore size of 3 nm, but Mizuno et al. [15] intruded mercury to that of 10 nm therefore, the actual total pore volume may be somewhat larger. Hamami et al. [12] measured the pore size distribution but showed the volume of the intruded mercury as the volume fraction versus the total pore volume; thus, the total pore volume cannot be read from the figure. Instead, the total pore volume measured as the weight difference of water-saturated and oven-dried samples is plotted in Fig. 4. The porosity measured by MIP is lower than that measured by the weight difference between water-saturated and oven-dried samples [40–42]. The determination coefficient of the air permeability coefficient and total pore volume is very low at 0.07. In Fig. 4, the results of concrete, mortar, and cement paste are included; concrete shows a lower total pore volume than cement paste because it includes aggregate. Therefore, it is preferable to use the total pore volume from the cement paste to study the correlation with air permeability. The total pore volume reported by Zhang et al. [13] is too large as a total pore volume of concrete. It is not stated in their paper, but it is likely that they calculated the total pore volume per cement paste volume. The total pore volume reported by Hilal et al. [33] is large because they studied foamed concrete samples. By removing the results of mortars and cement pastes (including those from Zhang et al. [13]) from Fig. 4, the determination coefficient becomes 0.32, which is still low. These results indicate that the total pore volume is not a good indicator of pore structure for determining the air permeability.

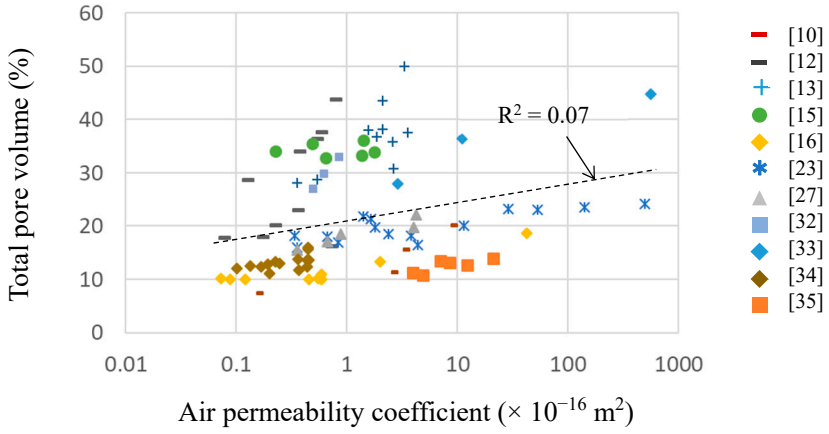

Fig. 4. Relationship between air permeability coefficient and total pore volume

Figs. 5 and 6 show the relationships of the air permeability coefficient with the critical pore diameter and threshold pore diameter, respectively. Their determination coefficients are moderate at 0.35 and 0.45, respectively. In some concrete samples, the threshold pore diameter cannot be determined because the sudden intrusion or inflection point is unclear, as in Fig. 3. Therefore, although the threshold pore diameter has been used often for cement pastes, it is not a good pore structure indicator for concretes. The relationship between the threshold pore diameter based on percolation theory [23] and the air permeability coefficient is shown in Fig. 7. The data of the foamed concrete [33] deviate from the approximation curve. The determination factor is high at 0.64. Fig. 8 shows the air permeability coefficient and the median pore diameter. The determination coefficient is 0.50, higher than those of the critical and ordinary threshold pore diameters. Similar to Fig. 7, the foamed concrete data deviate from the approximation curve. The critical and median pore diameters were reported to be similar [18,20], but their relationship in Fig. 9 shows the maximum difference of a few hundred times (two orders of magnitude). To determine the critical pore diameter, the maximum of the derivative of the pore size distribution curve must be identified; however, as seen in Fig. 2, this is not always easy, especially in concretes. However, the median pore diameter can be determined uniquely and shows better determination coefficients. These qualities support the median pore diameter as a better pore structure indicator for air permeability compared to the critical pore diameter. The data collected in this paper show that the threshold pore diameter based on percolation theory and median pore diameter are both good pore structure indicators for determining air permeability.

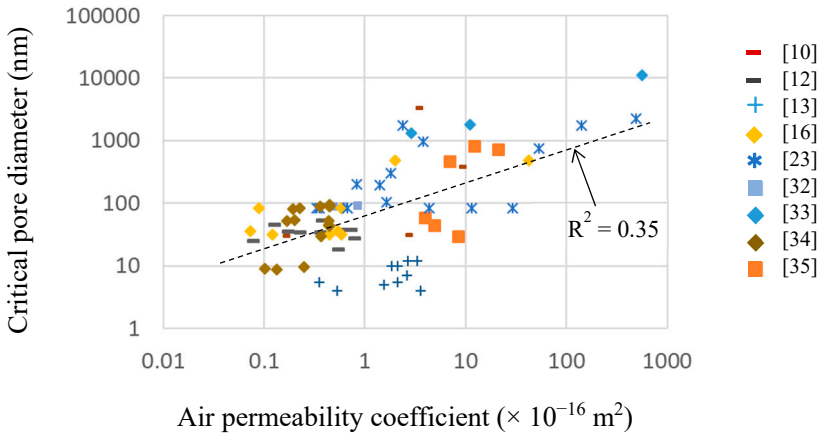

Fig. 5 Relationship between air permeability coefficient and critical pore diameter

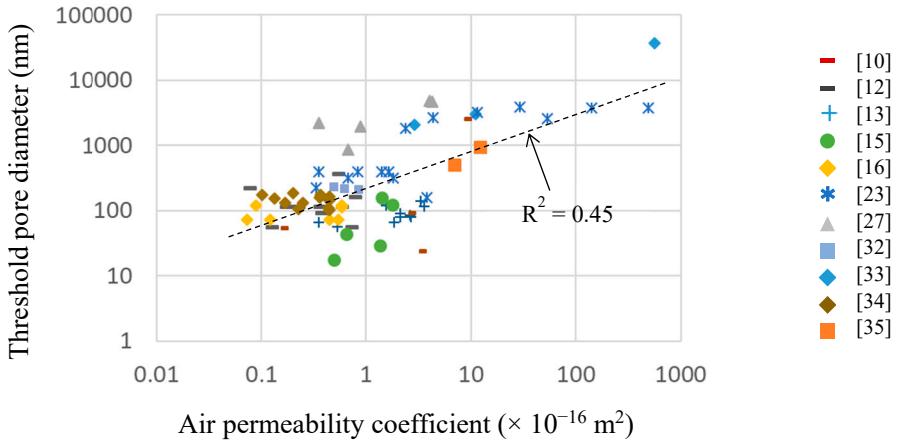

Fig. 6 Relationship between air permeability coefficient and threshold pore diameter determined by ordinary definition

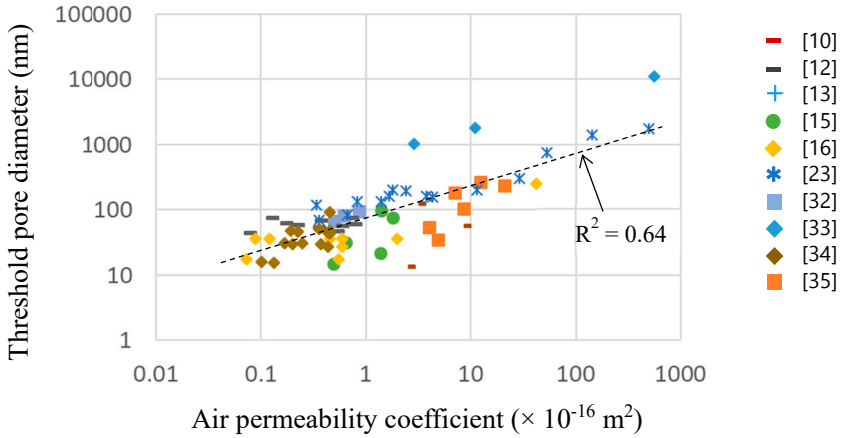

Fig. 7 Relationship between air permeability coefficient and threshold pore diameter as determined following the definition proposed by Sakai et al. [23]

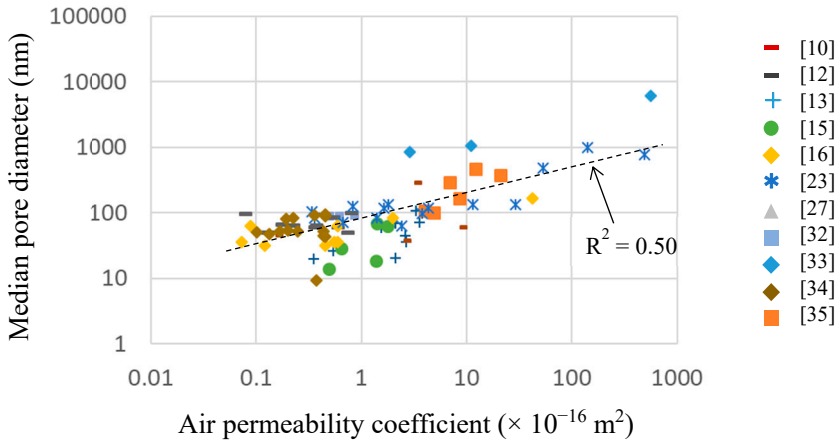

Fig. 8 Relationship between air permeability coefficient and median pore diameter

Preprints (www.preprints.org) | NOT PEER-REVIEWED | Posted: 6 December 2018 doi:10.20944/preprints201812.0078.v1

Peer-reviewed version available at Construction and Building Materials 2019, 209, 541-547; doi:10.1016/j.conbuildmat.2019.03.068

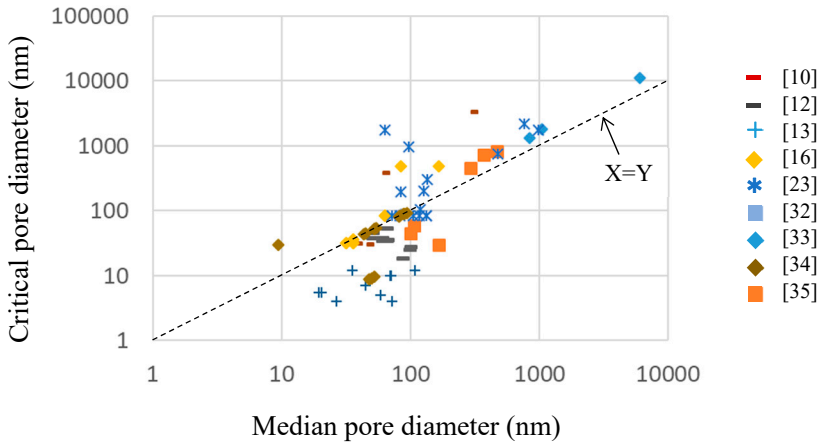

Fig. 9 Relationship between median pore diameter and critical pore diameter

Fig. 10 shows the relationship between the reported air permeability coefficients and the calculated permeability coefficients using the Katz–Thompson model [28,29]. The line in the figure indicates that the calculated and reported values are equal. The correlation appears reasonable, but some calculated values are several hundred times smaller than those measured. Ma [21] proposed the use of the characteristic pore diameter, instead of the critical pore diameter, when φ is <0.18, but the characteristic pore diameter is smaller than the critical pore diameter and this adjustment increases the deviation in Fig. 10. The exponential approximation of the relationship between the air permeability coefficient and the threshold pore diameter based on percolation theory is expressed as follows:

$$\text{Air permeability coefficient } [\times 10^{-16}\ \text{m}^2] = 0.005 \times (\text{Threshold pore diameter [nm]})^{1.26} \quad (6)$$

The calculated air permeability coefficients using this equation and the measured coefficients are shown in Fig. 11. The calculated and measured air permeability coefficients vary by the maximum factor of 10.

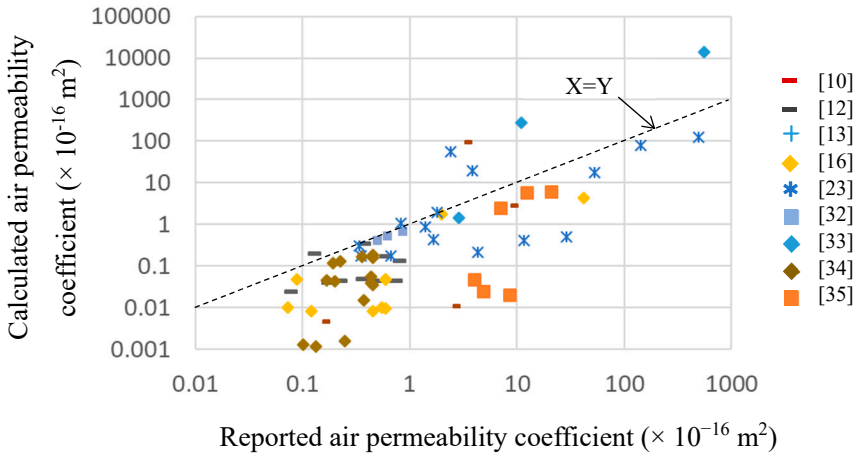

Fig. 10 Relationship between reported and calculated (Eqs. 2 and 3) air permeability coefficient

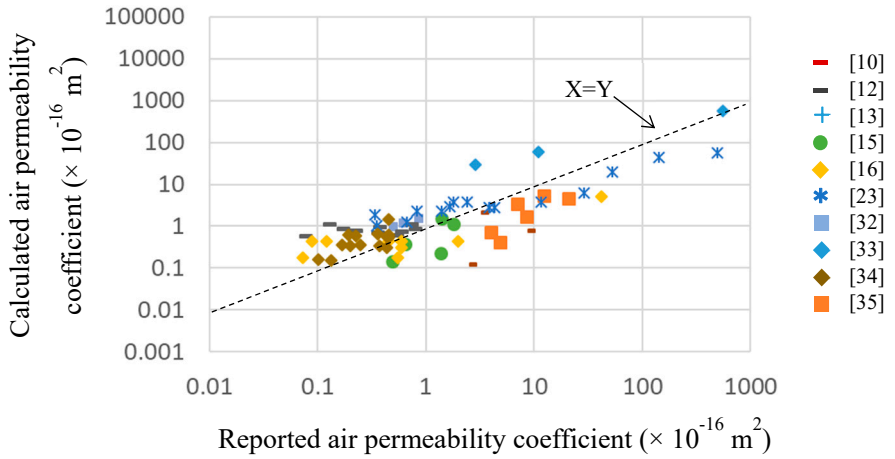

Fig. 11 Relationship between reported and calculated (Eq. 6) air permeability coefficient

The above results show that the air permeability coefficient calculated using the threshold pore diameter as defined based on percolation theory yields a better estimation than the commonly used Katz–Thompson model.

4. Conclusion

Previous reports measuring both the air permeability coefficients and pore structures of cementitious materials were collected to investigate the correlation of pore structure indicators with the air permeability coefficient and the validity of the equations used to estimate the air permeability coefficient. The total pore volume, critical pore diameter, and ordinary threshold pore diameter each showed poor correlation with the air permeability coefficient. However, the median pore diameter and the threshold pore diameter as defined based on percolation theory showed high correlations with the air permeability coefficient. An approximation curve to calculate the air permeability coefficient from the threshold pore diameter was derived, assuming an exponential relationship; the calculated result showed greater accuracy than the Katz–Thompson equation. Therefore, the results in this paper suggest the use of the median pore diameter or the threshold pore diameter based on percolation theory as an indicator of the pore structure that governs the air permeability of concrete, and the use of the approximation equation using the threshold pore diameter to estimate the air permeability coefficient based on the pore structure characteristics of the concrete.

Acknowledgements

This study was supported by JSPS KAKENHI grant number 18K13809.

References

[1] T. Sugiyama, T.W. Bremner, Y. Tsuji, Determination of chloride diffusion coefficient and gas permeability of concrete and their relationship, Cem. Concr. Res. 26(5) (1996) 781–790. https://doi.org/10.1016/S0008-8846(96)85015-0

[2] A. Abbas, M. Carcasses, J.P. Ollivier, The importance of gas permeability in addition to the compressive strength of concrete, Mag. Concr. Res. 52(1) (2000) 1–6. https://doi.org/10.1680/macr.2000.52.1.1

[3] K. Sasaki, H. Miyakoshi, Air and water permeabilities of coal ash and Portland cement mortars, Sci. Tech. Rep. Min. Coll., Akita Univ. (13) (1992) 1–8.

[4] R. Fujita, Importance of curing on concrete structures, J. Res. Comm. Minist. Land, Infrastruct. Transp., Chugoku Reg. Div. 61 (2010) 228–233.

[5] M.H. Kim, Y.J. Kwon, S.G. Park, S.P. Kang, An Experimental Study on the Permeability Coefficient Influencing to Carbonation of Mortar and Concrete, Proc. Jpn. Concr. Inst. 22(1) (2000) 193–198.

[6] K. Kurizuka, S. Tusunoda, N. Harada, Relationship between drying shrinkage and air permeability

coefficient of concrete, Proc. Annu. Conf. Jpn. Soc. Civ. Eng. 66 (2011) 547–548.
[7] L. Basheer, P.A.M. Basheer, A.E. Long, Influence of coarse aggregate on the permeation, durability and the microstructure characteristics of ordinary Portland cement concrete, Constr. Build. Mater. 19(9) (2005) 682–690. https://doi.org/10.1016/j.conbuildmat.2005.02.022
[8] H.S. Wong, R.W. Zimmerman, N.R. Buenfeld, Estimating the permeability of cement pastes and mortars using image analysis and effective medium theory, Cem. Concr. Res. 42(2) (2012) 476–483. https://doi.org/10.1016/j.cemconres.2011.11.018
[9] Y. Azuma, H. Mori, K. Tada, Influences of secondary wet curing on strength, durability and microstructure of steam cured mortar, Cem. Sci. Concr. Technol. 70(1) (2016) 405–412. https://doi.org/10.14250/cement.70.405
[10] D.N. Katpady, H. Hazehara, M. Soeda, T. Kubota, S. Murakami, Durability Assessment of Blended Concrete by Air Permeability, Int. J. Concr. Struct. Mater. 12(1) (2018) 30. https://doi.org/10.1186/s40069-018-0260-9
[11] S. Diamond, Mercury porosimetry: An inappropriate method for the measurement of pore size distributions in cement-based materials, Cem. Concr. Res. 30(10) (2000) 1517–1525. https://doi.org/10.1016/S0008-8846(00)00370-7
[12] A.A. Hamami, P. Turcry, A. Aït-Mokhtar, Influence of mix proportions on microstructure and gas permeability of cement pastes and mortars, Cem. Concr. Res. 42(2) (2012) 490–498. https://doi.org/10.1016/j.cemconres.2011.11.019
[13] X. Zhang, Z. Li, Q. Ma, X. Zhou, Q. Wang, Study on the correlation between SHPC pore structure and air permeability, Teh. Vjesn. 24(5) (2017) 1425–1430. https://doi.org/10.17559/TV-20170412102921
[14] S. Tsivilis, E. Chaniotakis, G. Batis, C. Meletiou, V. Kasselouri, G. Kakali, A. Sakellariou, G. Pavlakis, C. Psimadas, The effect of clinker and limestone quality on the gas permeability, water absorption and pore structure of limestone cement concrete, Cem. Concr, Compos. 21(2) (1999) 139–146. https://doi.org/10.1016/S0958-9465(98)00037-7
[15] K. Mizuno, R. Yoshida, H. Umehara, Relationship between compression strength, air permeability and pore structure of cementitious material with various replacement ratio of blast furnace slag, Proc. Jpn. Concr. Inst. 37(1) (2015) 523–528.
[16] Y. Sakai, T. Kishi, Establishment and validation of an indicator of pore structure that governs mass transport in concrete, Expressways and automobiles 57(10) (2014) 28–34.
[17] A.S. El-Dieb, R.D. Hooton, Evaluation of the Katz-Thompson model for estimating the water permeability of cement-based materials from mercury intrusion porosimetry data, Cem. Concr. Res. 24(3) (1994) 443–455. https://doi.org/10.1016/0008-8846(94)90131-7
[18] M.R. Nokken, R.D. Hooton, Using pore parameters to estimate permeability or conductivity of concrete, Mater. Struct. 41(1) (2007) 1. https://doi.org/10.1617/s11527-006-9212-y
[19] E.J. Garboczi, Permeability, diffusivity, and microstructural parameters: A critical review, Cem. Concr. Res. 20(4) (1990) 591–601. https://doi.org/10.1016/0008-8846(90)90101-3
[20] D.M. Roy, Relationships Between Permeability, Porosity, Diffusion And Microstructure Of Cement Pastes, Mortar, And Concrete At Different Temperatures, MRS Proc. 137 (2011) 179. https://doi.org/10.1557/PROC-137-179
[21] H. Ma, Mercury intrusion porosimetry in concrete technology: tips in measurement, pore structure parameter acquisition and application, J. Porous Mater. 21(2) (2014) 207–215. https://doi.org/10.1007/s10934-013-9765-4
[22] S. Mindess, J.F. Young, D. Darwin, Concrete, Prentice Hall, New Jersey, 2003.
[23] Y. Sakai, C. Nakamura, T. Kishi, Threshold pore radius of concrete obtained with two novel methods, in: D. Bjegović, H. Beushausen, M. Serdar (Eds.) RILEM International workshop on performance-based specification and control of concrete durability, Zagreb, Croatia, 2014.
[24] H. Scher, R. Zallen, Critical Density in Percolation Processes, J. Chem. Phys. 53(9) (1970) 3759–3761. https://doi.org/10.1063/1.1674565
[25] D.P. Bentz, E.J. Garboczi, Percolation of phases in a three-dimensional cement paste microstructural model, Cem. Concr. Res. 21(2) (1991) 325–344. https://doi.org/10.1016/0008-8846(91)90014-9
[26] P.C. Carman, Flow of gases through porous media, Academic Press, New York, 1956.
[27] S. Kohno, I. Ujike, Study on Change of Air Permeability Coefficient due to Drying, Proc. Jpn. Concr. Inst. 21(2) (1999) 847–852.
[28] A.J. Katz, A.H. Thompson, Quantitative prediction of permeability in porous rock, Phys. Rev.B 34(11) (1986) 8179–8181. https://doi.org/10.1103/PhysRevB.34.8179
[29] A.J. Katz, A.H. Thompson, Prediction of rock electrical conductivity from mercury injection

measurements, J. Geophys. Res. Solid Earth 92(B1) (1987) 599–607. https://doi.org/10.1029/JB092iB01p00599

[30] A.H. Thompson, A.J. Katz, C.E. Krohn, The microgeometry and transport properties of sedimentary rock, Adv. Phys. 36(5) (1987) 625–694. https://doi.org/10.1080/00018738700101062

[31] B.J. Christensen, T.O. Mason, H.M. Jennings, Comparison of measured and calculated permeabilities for hardened cement pastes, Cem. Concr. Res. 26(9) (1996) 1325–1334. https://doi.org/10.1016/0008-8846(96)00130-5

[32] H. Akiyama, T. Kishi, R. Yoshida, The effect of air entraining agent to pore size distribution and air permeability of hardened cement paste, Annual Conference of Japan Society of Civil Engineers, 2011, pp. 995–996.

[33] A.A. Hilal, N.H. Thom, A.R. Dawson, Pore Structure and Permeation Characteristics of Foamed Concrete, J. Adv. Concr. Technol. 12(12) (2014) 535–544. https://doi.org/10.3151/jact.12.535

[34] H. Nakase, M. Kakizaki, H. Edahiro, K. Fujii, Effect of pore structure of high-fluidity concrete to air and water permeabilities, Proc. Jpn. Concr. Inst. 16(1) (1994) 201–206.

[35] Y. Yokoyama, Y. Sakai, T. Kishi, Pore structure of middle scale column specimens exposed outdoors, Seisan Kenkyu, 2018 (accepted)

[36] F. Taguchi, A. Shimata, H. Shimada, I. Naito, S. Yoshida, H. Endo, M. Mizuta, K. Kawamura, S. Miyamoto, H. Sato, N. Nakamura, S. Shibuya, M. Watanabe, A study on the performance-based quality control and inspection methods for the construction of concrete structures, Report of important research project, Public Works Research Institute, 2014.

[37] S. Miyahara, T. Maruya, T. Kishi, Study on Improving the Durability of Concrete by Drainage and Underwater Curing, Report of Taisei Technology Center 44 (2011) 24-1–24-7.

[38] L. Basheer, J. Kropp, D.J. Cleland, Assessment of the durability of concrete from its permeation properties: a review, Constr. Build. Mater. 15(2) (2001) 93–103. https://doi.org/10.1016/S0950-0618(00)00058-1

[39] Y. Sakai, Numerical study on the relationship among air permeability, pore size and pressure assuming molecular and viscous flows, J. Adv. Concr. Technol. 15(3) (2017) 103–109. https://doi.org/10.3151/jact.15.103

[40] A.B. Auskern, W.H. Horn, Effect of curing conditions on the capillary porosity of hardened Portland cement pastes, J. Am. Ceram. Soc. 59(1-2) (1976) 29–33. https://doi.org/10.1111/j.1151-2916.1976.tb09380.x

[41] K. Kurumisawa, T. Nawa, Electrical Conductivity and Chloride Ingress in Hardened Cement Paste, J. Adv. Concr. Technol. 14(3) (2016) 87–94. https://doi.org/10.3151/jact.14.87

[42] J.P. Ollivier, M. Torrenti, M. Carcassès, Physical Properties of Concrete and Concrete Constituents, Wiley, London, UK, 2012.